Click Chemistry on NiO Photocathode to Postfunctionalize a Diketopyrrolopyrrole Sensitizer by Naphthalene Diimide Electron Acceptor

Yousra Bentounsi, Konstantinos Seintis, Stéphane Diring, Eric Vauthey, Fabrice Odobel

Click chemistry on NiO photocathode to post-functionalize a diketopyrrolopyrrole sensitizer by naphthalene diimide electron acceptor

Yousra Bentounsi,[a] Konstantinos Seintis,[b] Stéphane Diring,[a] Eric Vauthey[b] Fabrice Odobel*[a]*

[a]Université de Nantes, CNRS, CEISAM UMR 6230, F-44000 Nantes, France. E-mail: Fabrice.Odobel@univ-nantes.fr
Department of Physical Chemistry, University of Geneva, 30 Quai Ernest-Ansermet, CH-1211 Geneva, Switzerland. E-mail: Eric.Vauthey@unige.ch

Abstract:

This study addresses a practical aspect of hybrid dye-sensitized photoelectrochemical cells by exploring a simple method to prepare multicomponent systems. Building on a previously reported methodology based on a copper-free click chemistry dipolar cycloaddition of azide with activated alkyne, a naphthalene diimide (NDI) derivative substituted with two propiolic esters was clicked on a NiO photocathode already coated with a diketopyrrolopyrrole (DPP) dye bearing two azido groups. A detailed photophysical study by transient absorption spectroscopy demonstrates that optical excitation of DPP dye leads to an effective electron transfer chain from the NiO valence band to the NDI passing *via* the DPP dye, resulting to a long-lived charge-separated state (hole in NiO/NDI radical anion) of 170 μs. p-type dye-sensitized solar cells were also fabricated with the above molecular components and confirm the occurrence of the electron transfer as the performances of the solar cells were improved in terms of Voc and Jsc compared to the DPP dye lacking the NDI unit. The above clicked system was also compared to a covalently linked DPP-NDI dyad, whose performances are 30% superior to the clicked system probably due to longer mean distance between the NiO surface and the NDI with the dyad. This finding paves the way for the design of multicomponent hybrid dye-sensitized photoelectrochemical cells by chemistry on the electrode.

Introduction

Hybrid nanomaterials consisting of a nanocrystalline metal oxide film whose surface area is coated with a molecular system are the key components of dye-sensitized solar cells (DSSCs),[1] dye-sensitized photoelectrosynthetic cells (DSPECs)[2, 3, 4] and even other electronic devices.[5, 6] So far, many studies on dye-sensitized photoelectrochemical cells have mostly focused on the design of more efficient sensitizers[1, 7] or catalysts,[8, 9] but they are very few works devoted to the development of versatile and powerful fabrication techniques to assemble several molecular components on the surface of mesoporous metal oxide films. On one hand, copper-catalyzed click chemistry between an azide and a terminal alkyne is a classical strategy to functionalize surfaces.[10, 11] Notable examples of this approach are the modification of flat surfaces of gold[12] and silica,[13] of spherical nanoparticles,[14] and even mesoporous metal oxide layers.[15, 16, 17, 18] Except for the recent elegant works of Dinolfo and co-workers on flat ITO substrates,[19, 20] surface post-functionalization is, however, often limited to the immobilization of a single molecular component *via* a simple alkyl chain terminated by azido or alkyne group and grafted on the surface *via* a carboxylic or alkoxysilane anchoring group. On the other hand, it is well accepted that molecular complexity is a prerequisite to achieve elaborated functions. In this context, preformed bi-component molecular systems, such as "dye-catalyst" systems for DSPECs, have been prepared prior immobilization on the surface, but they require tedious, multistep procedures and complex chromatographic separations.[3, 4, 21, 22, 23] A bottom-up approach that permits the straightforward functionalization of a porous film by the successive grafting of different molecular components onto each other would be extremely useful to achieve complex functionalities such as highly active photocatalytic systems and even beyond, but they are rare and particularly on mesoporous electrodes. Meyer and co-workers have reported two interesting strategies toward this goal. One is based on the reductive electro co-polymerization of vinyl groups born by the dye and an oxidation catalyst[24, 25, 26] and the other method makes use of phosphonate chemistry between the free phosphonic acid groups on a dye and a catalyst which are assembled *via* a zirconium(IV) cation.[27] In the same vein, more recently Tian and Hammarström have used the amide-coupling reaction to attach catalysts on a silatrane-decorated NiO photocathode.[28, 29] Building on an innovative copper-free click chemistry strategy,[30] which proved very efficient to stabilize the dye from the desorption from the electrode, we investigate herein the possibility to implement this strategy to post-functionalize the photoelectrode with an active component to fabricate a photoactive hybrid system in view of obtaining a more elaborate property (Scheme 1). More specifically, we have explored the opportunity to introduction of a naphthalene diimide (NDI) electron acceptor by click chemistry on the already chemisorbed DPP layer on NiO electrode in order slow down the usually fast geminate charge recombination reaction.

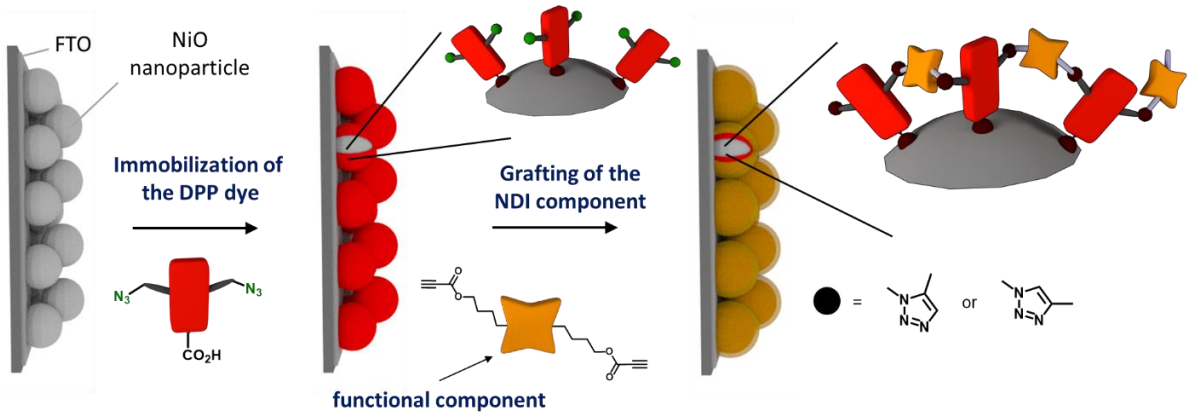

Scheme 1. Schematic representation of the click chemistry reaction directly conducted on NiO nanocrystalline electrode with symbolic representation of the DPP dye (red) and NDI electron acceptor (yellow star).

It is well accepted that charge recombination is one of the major causes of the low performances of p-DSSCs and the introduction of a secondary electron acceptor to the sensitizer is an effective strategy to overcome this problem.[31, 32, 33, 34] Moreover, in p-DSPEC it is crucial to efficiently shuttle several reducing equivalents produced on the dyes to activate the catalysts prior the catalytic event. Our objective in this study was, therefore, to explore if the post-functionalization of the DPP dye by copper-free click reaction with NDI could be compatible with the effective electron transfer from DPP to this secondary electron acceptor. In case of success, this would pave the way to the straightforward incorporation of many reduction catalysts for the fabrication of DSPECs. Toward this end, we have prepared the new **NDI**, which was clicked to the **DPP** dye after its chemisorption on NiO electrode (Chart and Scheme 1). The previously reported dyad **DPP-NDI**[34] was also studied for comparison purposes. The photophysical study by transient absorption spectroscopy and the photovoltaic measurements clearly evidence that the electron-transfer chain from the valence band of NiO to the NDI *via* the photoexcited DPP effectively occurred in the clicked assembly.

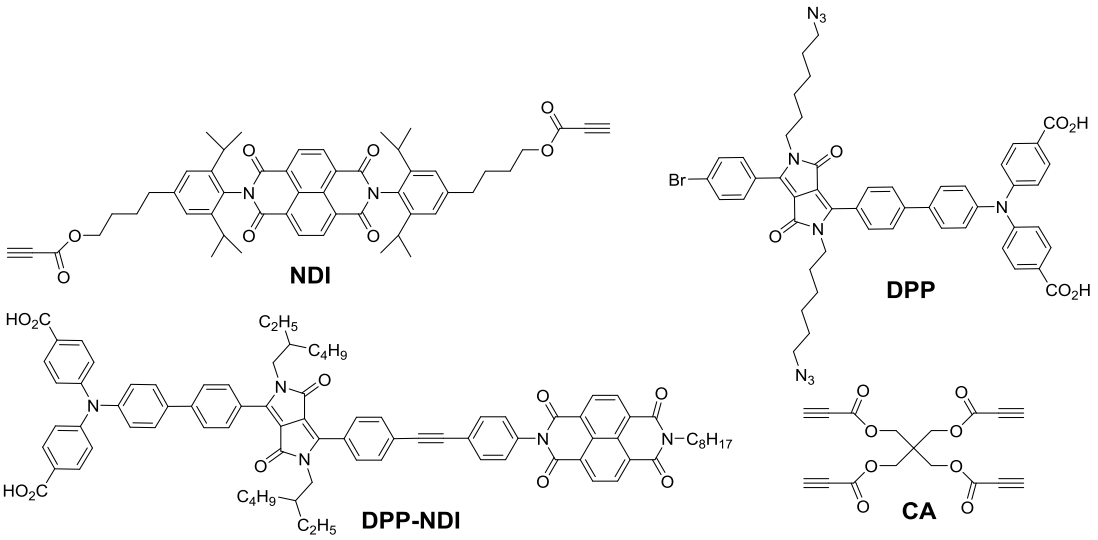

Chart. Structures of the components investigated in this work.

Fabrication of the assembly on mesoporous electrode

The synthetic route of the **NDI** is illustrated on Scheme 2. In brief, 4-iodo-2,6-diisopropylaniline **1** was coupled to 3-butyn-1-ol according to a Sonogashira cross-coupling reaction and the triple bond was reduced quantitatively with hydrogen on palladium on charcoal to afford the aniline derivative **3**. The latter aniline **3** was condensed in refluxed acetic acid with naphthalenetetracarboxylic dianhydride to afford the naphthalene diimide **4** in which the alcohol groups were esterified into acetate. This was not an issue, since the acetate groups can be subsequently trans-esterified by 3-(trimethylsilyl) propiolic acid in good yield (87%) in the next step. Finally, the trimethylsilyl (TMS) protecting groups were cleaved by tetrabutylammonium fluoride (TFA) in almost quantitative yield to give **NDI**.

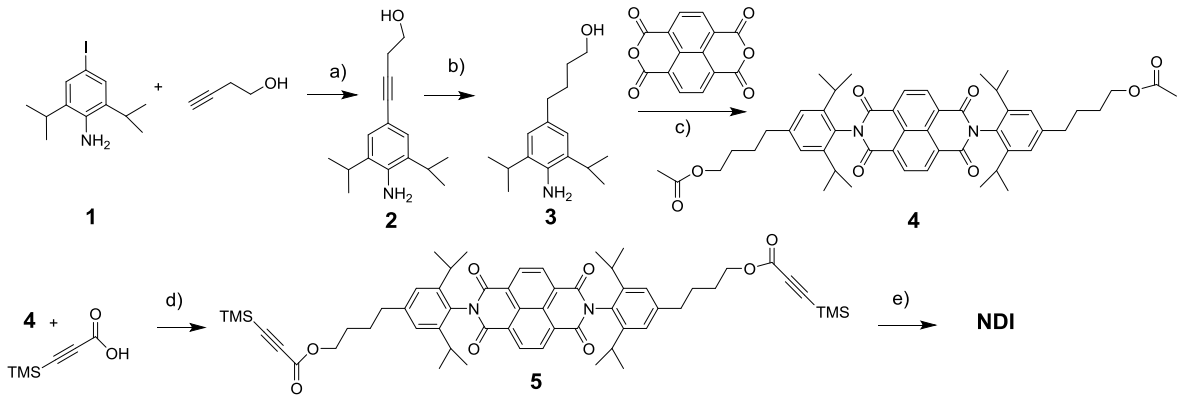

Scheme 2. Synthetic scheme for **NDI**. Reagents and conditions: a) $Pd(PPh_3)_2Cl_2$, CuI, Et_2NH/THF (1/2), RT, 12h, 70%; b) 10%-Pd/C, AcOEt, RT, 12h, 99%; c) acetic acid, 120 °C, 12h, 54%; d) APTS, benzene, 90 °C, 5d, 87%; e) TBAF, acetic acid, THF, RT, 30min, 99%.

The **NDI** was connected to the **DPP** dye already grafted on nanocrystalline NiO electrode by click reaction by a simple heating at 140°C for 20 minutes of the NiO photocathode into an orthodicholorobenzene solution of **NDI** (see ESI materials for detailed experimental conditions). We have previously demonstrated that these conditions exclusively lead to Huisgen cycloaddition product as schematically shown in Scheme 1.[30] The reaction was monitored by ATR-IR spectroscopy (Figure 1). The NDI displays characteristic IR bands located around 1717 cm^{-1} and 1675 cm^{-1} for asymmetric and symmetric stretching band of carbonyl group on diimide and the also intense C–N–C absorption at 1340 cm^{-1}.[35] Moreover, the carbonyl group of propiolate ester is located around 1708 cm^{-1} and that of the lactam of DPP at 1676 cm^{-1}.[30] The ethynyl stretching band at 2118 cm^{-1} of **NDI** completely collapsed after heating while that of the azido at 2098 cm^{-1} has strongly shrunk, evidencing thus that most of these two reacting groups have been consumed during the functionalization process. Interestingly, after click reaction and abundant rinsing of the photocathode, the carbonyl stretching band of diimide groups in **NDI** and of the propiolate ester around 1710 cm^{-1} appeared next to that of the lactam groups of **DPP** at 1670 cm^{-1} accounting for the covalent attachment of the NDI to the DPP dye (Figure 1).

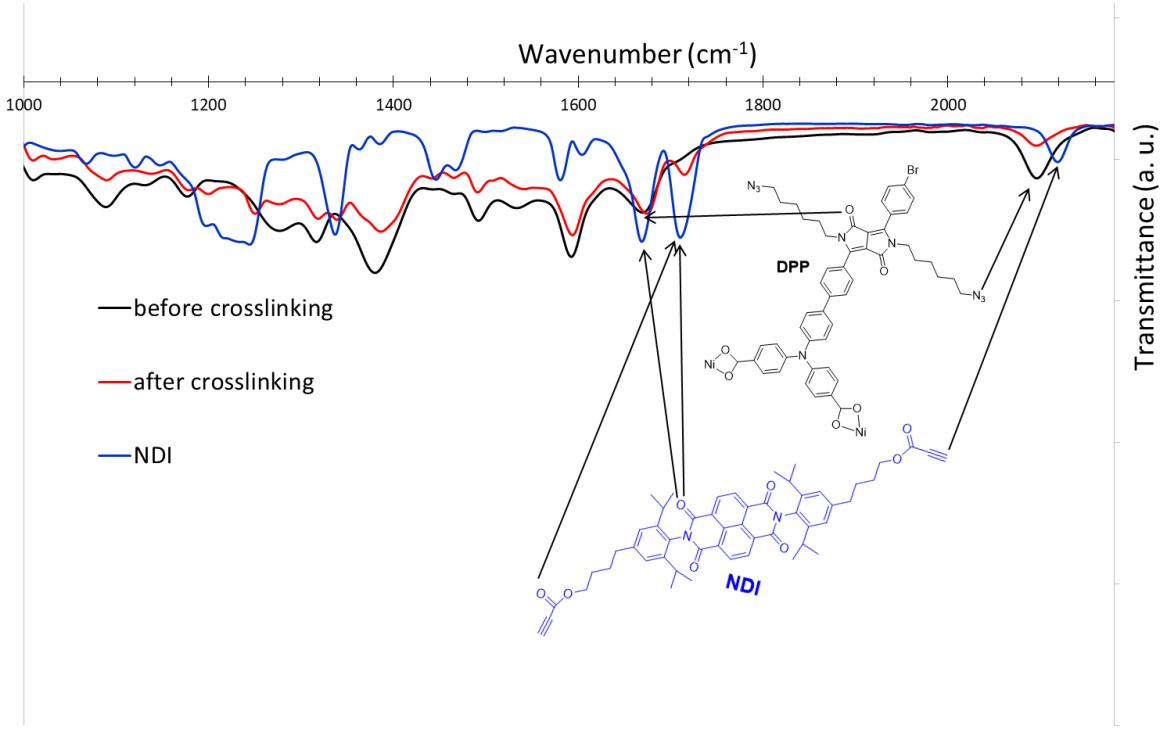

Figure 1. ATR-IR spectra of **NDI** powder (blue) and of the NiO electrodes coated with **DPP** before (black) and after click reaction with **NDI** (red).

Table 1. Spectroscopic and electrochemical data of the compounds and Gibbs free energy for the hole injection into NiO (ΔG_{hinj}) and for the dye regeneration reaction (ΔG_{reg}) by the cobalt electrolyte.

	$\lambda_{abs}/\varepsilon$ (nm/M^{-1}xcm^{-1})	E_{00} (eV)[a]	E_{Red}(NDI/NDI^-) (V *vs.* SCE)	E_{Red}(DPP/DPP^-) (V *vs.* SCE)	ΔG_{hinj} (eV)[b]	ΔG_{reg} (eV)[c]
DPP[d]	489 (2.22x10^4)	2.33	-	-1.20 V	-0.83	-1.41
NDI	362 (2.54x10^4); 382 (2.82x10^4)	-	-0.52 V	-	-	-
DPP-NDI[e]	380 (5.08x10^4); 492 (2.20x10^4)	2.29	-0.60 V	-1.22 V	-0.77	-0.81

[a]calculated according to the equation: E_{00} = 1240/ λ_{inter}, with λ_{inter} the wavelength at the intersection of the normalized absorption and emission spectra. [b]Calculated according to the equation: $\Delta G°_{inj}$ = E_{BV}(NiO) - E_{Red}(DPP/DPP^-) with E_{Red}(DPP*/DPP^-) = E_{Red}(DPP/DPP^-) + E_{00} and E_{BV}(NiO) = 0.30 V *vs* SCE. [c]Calculated according to the equation: ΔG_{reg}= E_{Red}(A/A^-) - E(Co^{III}/Co^{II}) with A = DPP or NDI and E(Co^{III}/Co^{II}) = 0.21 V *vs.* SCE. [d]data taken from ref. [30]. [e]data taken from ref. [34].

The electronic absorption spectra were also recorded on mesoporous Al_2O_3 electrodes, because the transparency of Al_2O_3 films is much higher than that of NiO films.[36, 37] After the click reaction, the π-π* transition of **NDI** is clearly discernible in the spectrum as a shoulder at 380 nm and its relative intensity matches very well with that of the **DPP-NDI** dyad (Figure 2). The extinction coefficient of the DPP in both compounds (**DPP** and **DPP-NDI**) being very similar, the comparison of the absorption spectra on mesoporous Al_2O_3 of **DPP** clicked with **NDI** with that of the **DPP-NDI** dyad qualitatively indicates that there is be about one **NDI** unit per **DPP** dye after the click reaction. The absorption band of DPP chromophore (around 500 m) is slightly red shifted in **DPP-NDI** compared to that of **DPP** because of the increased π-conjugation upon connection of NDI *via* the triple bond.[34]

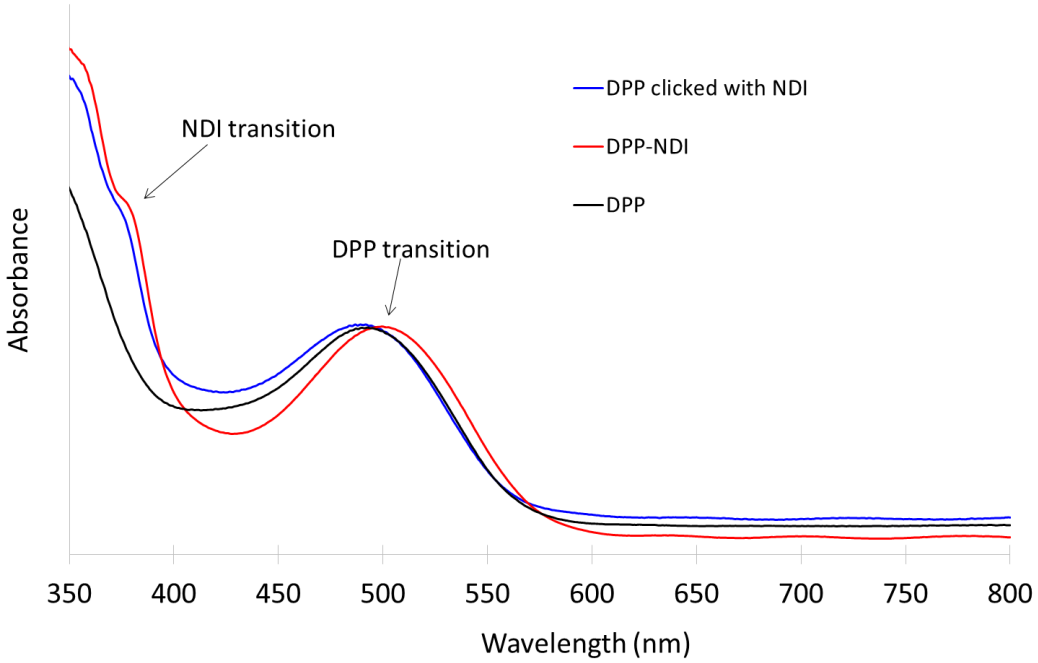

Figure 2. *Normalized absorption spectra of Al_2O_3 films coated with* ***DPP-NDI*** *(red),* ***DPP*** *before (black) and after click reaction with* ***NDI*** *(blue). The three spectra were normalized on the DPP absorption band.*

The spectroscopic and electrochemical data of the compounds are gathered in Table 1. The determination of the driving forces for the hole injection process into the valence band of NiO and the regeneration reaction of the reduced dye by the redox mediator in the electrolyte were calculated (Table 1). Unsurprisingly, they support that these two reactions are both thermodynamically very favorable and therefore can occur spontaneously.

Photophysical study

The excited-state dynamics of **DPP**, **DPP-NDI** and **DPP** crosslinked with **NDI** on NiO were investigated from the femtosecond to the microsecond timescales using electronic transient absorption (TA) spectroscopy to determine the charge-transfer processes taking place upon excitation of the DPP dye at 532 nm.[34, 38, 39]

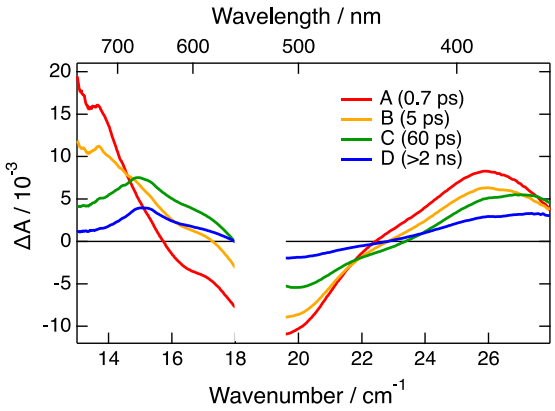

Figure 3. *Evolution-associated difference absorption spectra (EADS) obtained upon global analysis of the transient absorption data measured after 532 nm excitation of* ***DPP*** *on NiO assuming a series of successive exponential steps (A→...→D→)*

As discussed previously,[30] the excited-state dynamic of **DPP**, grafted NiO with or without crosslinking with **CA** are essentially the same. Figure 3 shows the evolution-associated difference absorption spectra (EADS)[40, 41] obtained from a global analysis of the TA data measured with **DPP** on NiO after 532 nm excitation assuming a series of successive exponential steps with increasing time constants (see Figure S1 for the data). Directly after excitation of **DPP**, the TA spectra show positive absorption bands of the singlet excited state of the DPP sub-unit, DPP*(S_1), at 730 and 390 nm as well as a negative band between 430 and 620 nm that is due to both the ground-state bleach around 500 nm and the stimulated emission at longer wavelengths. The latter decays in a few picoseconds, whereas the 730 nm band evolves into a band centered around 660 nm that can be attributed to the radical anion of DPP generated upon hole injection into NiO.[42] This band losses about half of its maximum intensity with a 60 ps time constant and then decays on a 2-3 ns timescale. An average charge injection time constant of about 2-3 ps can be estimated from the decay of the DPP excited state.

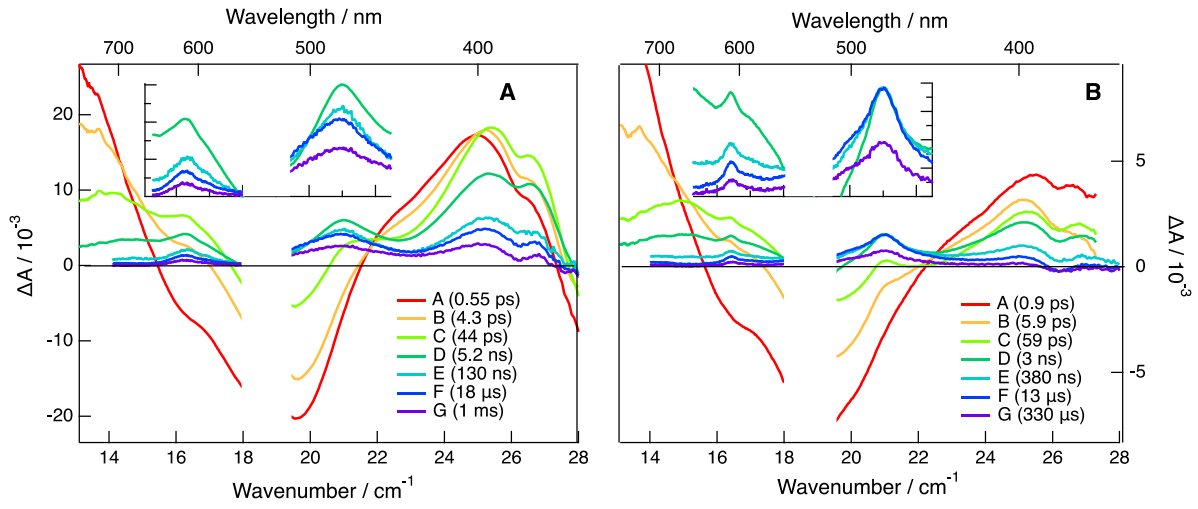

Figure 4. *Evolution-associated difference absorption spectra (EADS) obtained upon global analysis of the transient absorption data measured after 532 nm excitation of A)* ***DPP-NDI*** *and B)* ***DPP*** *crosslinked with* ***NDI*** *on NiO, assuming a series of successive exponential steps (A→...→G→). Inset: zoom-in of EADS D-G. The values in parentheses are the decay times of the corresponding EADS.*

Figure 4A shows the EADS obtained from a global analysis of the TA data measured on the femtosecond to microsecond timescales with **DPP-NDI** grafted on NiO after 532 nm excitations (see Figure S2-3 for the data). The early spectra are essentially the same as those measured at short time delays with **DPP** (Figure 3) and can, thus, be assigned to the DPP subunit locally excited in the S_1 state, DPP*(S_1). These features decay on multiple timescales ranging from less than 1 ps to a few ps (EADS A-C). In parallel, distinct maxima appear around 700 and 600 nm. They can be attributed to the radical anion of the DPP and NDI subunits, respectively in agreement with previous works.[34, 42, 43] Additionally, the positive band, initially at 400 nm, shifts to shorter wavelength and a dip around 380 nm, that can be assigned to the bleach of the NDI subunit, becomes visible. The overlap of this positive feature with bleaches around 380 nm and a below 370 nm makes the assignment of this band difficult. From the time dependence of its relative intensity, it probably contains contributions from both DPP·$^-$ and NDI·$^-$ after the decay of DPP*(S_1).[34] The attribution of the 700 nm band in EADS C to DPP·$^-$ is supported by the absence of stimulated emission and the relatively strong DPP bleach that hides the 480 nm band of NDI·$^-$. By going from EADS C to D, the decrease of DPP·$^-$ band is accompanied by the decay of the DPP bleach and the appearance of NDI·$^-$ band at 480 nm. Therefore, hole injection from DPP*(S_1) to NiO takes place during the A→C (0.55 ps, 4.3 ps) steps, whereas the C→D (44 ps) step mostly reflects the shift of the electron from the DPP to the NDI subunit. Due to the inhomogeneity of the dynamics, this shift is also visible in the B→C (4.3 ps) step as the rise of the 600 nm band of NDI·$^-$ as well as in the slower D→E (5.2 ns) step. After about 10 ns,

the overall shape of the TA spectrum remains mostly constant and is dominated by the NDI·⁻ bands. Their decay can be reproduced using the sum of three exponential functions with 130 ns, 18 μs and ~ 1 ms time constants, giving an average decay time of about 550 μs.

As illustrated by the EADS depicted in Figure 4B (see Figure S4-5 for the data), the TA spectra measured with **DPP** crosslinked with **NDI** on NiO exhibit similar features than those measured with the **DPP-NDI** dyad (Figure 4A). From the global analysis, it appears that hole injection occurs on similar timescale (A→C steps with 0.9 and 5.9 ps time constants) than with the dyad. The presence of DPP·⁻ in EADS C and D is more visible than for the dyad. This can be explained by a slightly slower electron shift to the NDI in the crosslinked system (59 ps vs 44 ps), allowing for a larger accumulation of the DPP·⁻ population. This longer lifetime of DPP·⁻ is visible as a slower rise of the NDI·⁻ absorption band at 480 nm (Figure 5).

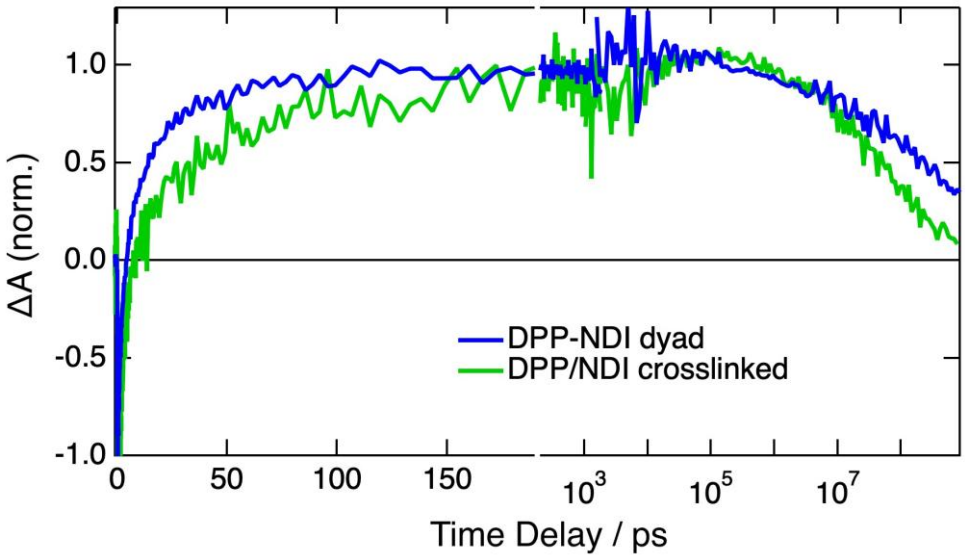

Figure 5. *Time profiles of the transient absorption at 480 nm, the maximum of NDI·⁻ absorption band, after excitation of* ***DPP-NDI*** *and* ***DPP*** *crosslinked with* ***NDI*** *on NiO.*

After about 10 ns, the TA spectra show only features due to NDI·⁻. The decay of the main NDI·⁻ band at 480 nm can be reproduced with the sum of two exponential functions with 13 and 330 μs time constant, corresponding to an average decay time of 170 μs. This points to a somewhat faster recombination dynamics than for the dyad (Figure 5). This can be explained most reasonably by a shorter mean distance between the NDI and the NiO surface when the latter is linked on the DPP *via* click chemistry. Figure 6 summarizes the main results of this photophysical study.

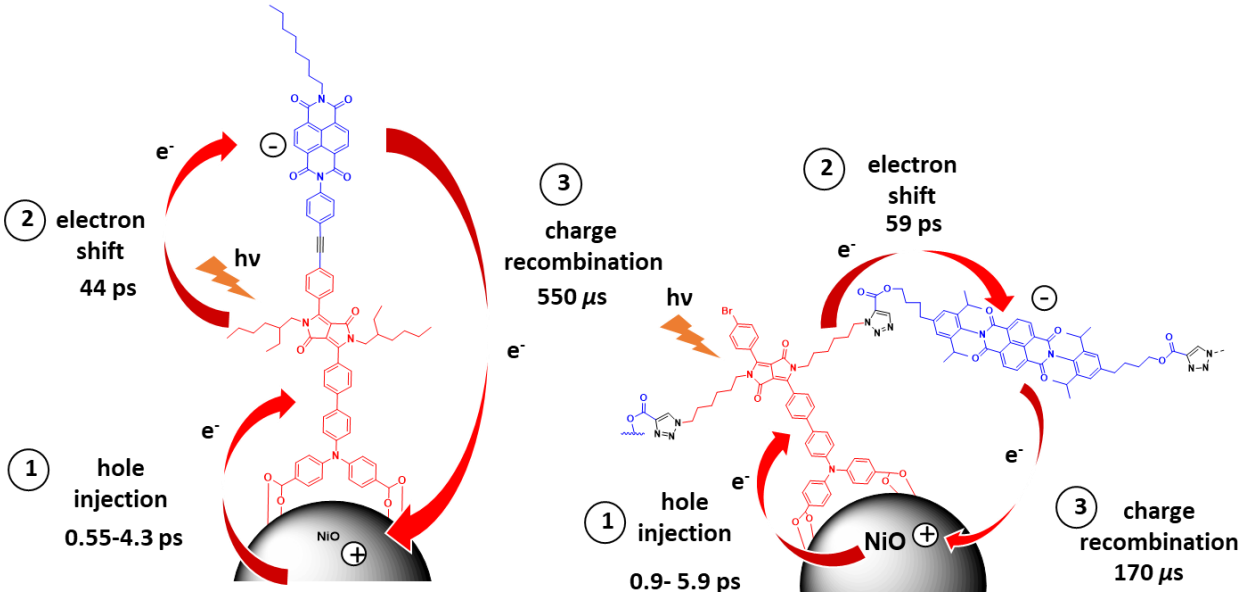

Figure 6. *Graphical summary of the main rate constants of the charge transfer processes occurring upon photoexcitation of the DPP dye in the two systems.*

Photovoltaic properties

Solar cells were fabricated on nanocrystalline film of NiO with **DPP** without and after introduction of **NDI** by click chemistry and the characteristics of the p-DSSCs were compared to those of the **DPP-NDI** and **DPP** cross-linked with the passive tetraalkyne (cross-linking agent : **CA** Chart). The tris(4,4'-diterbutyl-2,2'-bipyridine) cobalt complex was used as redox mediator (Figure S6), because this specific redox couple demands a long-lived charge-separated state, enabling thus to indirectly probe the enhancement of the charge-separated state lifetime with NDI. [32, 44 31] The metrics from at least three independent solar cells, such as short circuit current density (Jsc), open circuit voltage (Voc), fill factor (ff) and power conversion efficiency (PCE) are gathered in Table 2. Typical current/voltage curves are shown in Figure S7.

Table 2. Metrics of the solar cells recorded under calibrated AM1.5 (100 mW/cm^2) sunlight simulator.

	J_{SC} (mA/cm^2)	V_{OC} (mV)	FF (%)	PCE (%)
DPP	0.88±0.08	133±6	25±2	0.023±0.004
DPP crosslinked with **CA**	0.87±0.1	200±5	28±1	0.048±0.008
DPP crosslinked with **NDI**	1.40±0.07	254±8	32±1	0.10±0.008
DPP-NDI	1.94±0.05	340±8	31±0.7	0.205±0.003

The comparison of the characteristics of the solar cells sensitized with the **DPP** without and after cross-linked with the passive tetraalkyne **CA** shows that the Jsc was not modified, but the Voc was significantly increased. This is certainly due to the physical barrier brought by the crosslinking agent, which bridges the DPP and most certainly restricts the approach of the redox mediator to the NiO surface.[30] As a result, the interfacial charge recombinations are reduced and the hole concentration in the NiO valence band is higher, explaining thus the larger Voc. Interfacial charge recombination reaction is important in p-DSSC and particularly with the one electron outer-sphere redox mediator such as cobalt complexes.[32, 44] The introduction of NDI electron acceptor by click reaction in the film has a real beneficial impact over the passive **CA** since both Jsc and Voc are raised. These changes are the direct consequence of the longer-lived charge-separated state (hole in NiO and electron on NDI) formed upon electron shift from the reduced DPP to the clicked **NDI** as demonstrated above by the transient absorption. The comparison of the performances of the solar cells made with the dyad **DPP-NDI** and the system in which **NDI** was clicked on **DPP** shows that the Jsc and Voc are slightly higher with the dyad. However, the superiority of the dyad is not huge (30%). This result can be explained by the longer-lived charge-separated state achieved with the dyad, probably due to the longer average distance between the NDI and the NiO surface.

Conclusion

The present work provides a successful illustration of the post-functionalization of a dye-sensitized photocathode *via* a copper-free click chemistry by a NDI electron acceptor. The NDI component can be grafted on the DPP dye according to a simple procedure and the electron shift reaction from the reduced **DPP** and **NDI** occurs with a good efficiency as confirmed by the photophysical study and the photovoltaic measurements on p-DSSCs. This click reaction is probably compatible with a wide range of molecular components such as catalysts and other dyes to enhance light capture by antenna effect.[45] This work shows that the chemistry on the electrode *via* this simple click chemistry strategy has great potential for the straightforward modification of mesoporous metal oxide electrodes, and can represent a significant leap forward in the development of dye-sensitized electrochemical systems.

Acknowledgements: Région des Pays de la Loire is gratefully acknowledged for the financial support of these researches through the project "ClickChemHybrids" *via* the program LUMOMAT. The authors greatly acknowledge J. Hémez and L. Arzel (AMaCC platform, CEISAM UMR CNRS 6230, University of Nantes) for the mass spectrometry analyses. EV thanks the Swiss National Science Foundation (grant 200020-184607) and the University of Geneva for financial support.

Supporting information available: Synthesis of the NDI, preparation and characterizations of the DSSCs, additional transient absorption spectroscopy spectra, current/voltage characteristics of the solar cells, and ^{1}H and ^{13}C spectra of the new compounds. The transient absorption data can be downloaded from https://doi.org/10.26037/yareta:3byyprcnrzd67d5mja3xndytdy

References:

(1) Hagfeldt, A.; Boschloo, G.; Sun, L.; Kloo, L.; Pettersson, H. Dye-Sensitized Solar Cells. *Chem. Rev.* **2010,** *110*, 6595-6663.
(2) Yu, Z.; Li, F.; Sun, L. Recent advances in dye-sensitized photoelectrochemical cells for solar hydrogen production based on molecular components. *Energy Environ. Sci.* **2015,** *8*, 760-775.
(3) Gibson, E. A. Dye-sensitized photocathodes for H2 evolution. *Chem. Soc. Rev.* **2017,** *46*, 6194-6209.
(4) Ashford, D. L.; Gish, M. K.; Vannucci, A. K.; Brennaman, M. K.; Templeton, J. L.; Papanikolas, J. M.; Meyer, T. J. Molecular Chromophore-Catalyst Assemblies for Solar Fuel Applications. *Chemical Reviews (Washington, DC, United States)* **2015,** *115*, 13006-13049.

(5) Yu, M.; Ren, X.; Ma, L.; Wu, Y. Integrating a redox-coupled dye-sensitized photoelectrode into a lithium-oxygen battery for photoassisted charging. *Nat. Commun.* **2014,** *5*, ncomms9103.
(6) Nagashima, T.; Ozawa, H.; Suzuki, T.; Nakabayashi, T.; Kanaizuka, K.; Haga, M.-a. Photoresponsive Molecular Memory Films Composed of Sequentially Assembled Heterolayers Containing Ruthenium Complexes. *Chem. Eur. J.* **2016,** *22*, 1658-1667.
(7) Nikolaou, V.; Charisiadis, A.; Charalambidis, G.; Coutsolelos, A. G.; Odobel, F. Recent advances and insights in dye-sensitized NiO photocathodes for photovoltaic devices. *J. Mater. Chem. A* **2017,** *5*, 21077-21113.
(8) Dalle, K. E.; Warnan, J.; Leung, J. J.; Reuillard, B.; Karmel, I. S.; Reisner, E. Electro- and Solar-Driven Fuel Synthesis with First Row Transition Metal Complexes. *Chemical Reviews (Washington, DC, United States)* **2019,** *119*, 2752-2875.
(9) Matheu, R.; Ertem, M. Z.; Gimbert-Suriñach, C.; Sala, X.; Llobet, A. Seven Coordinated Molecular Ruthenium–Water Oxidation Catalysts: A Coordination Chemistry Journey. *Chemical Reviews (Washington, DC, United States)* **2019,** *119*, 3453-3471.
(10) Binder, W. H.; Sachsenhofer, R. 'Click' Chemistry in Polymer and Materials Science. *Macromolecular Rapid Commun.* **2007,** *28*, 15-54.
(11) Meldal, M.; Tornøe, C. W. Cu-Catalyzed Azide−Alkyne Cycloaddition. *Chem. Rev.* **2008,** *108*, 2952-3015.
(12) Lee, J. K.; Chi, Y. S.; Choi, I. S. Reactivity of Acetylenyl-Terminated Self-Assembled Monolayers on Gold: Triazole Formation. *Langmuir* **2004,** *20*, 3844-3847.
(13) Lummerstorfer, T.; Hoffmann, H. Click Chemistry on Surfaces: 1,3-Dipolar Cycloaddition Reactions of Azide-Terminated Monolayers on Silica. *J. Phys. Chem. B* **2004,** *108*, 3963-3966.
(14) White, M. A.; Johnson, J. A.; Koberstein, J. T.; Turro, N. J. Toward the Syntheses of Universal Ligands for Metal Oxide Surfaces: Controlling Surface Functionality through Click Chemistry. *J. Am. Chem. Soc.* **2006,** *128*, 11356-11357.
(15) Wu, L.; Eberhart, M.; Shan, B.; Nayak, A.; Brennaman, M. K.; Miller, A. J. M.; Shao, J.; Meyer, T. J. Stable Molecular Surface Modification of Nanostructured, Mesoporous Metal Oxide Photoanodes by Silane and Click Chemistry. *ACS Appl. Mater. Interfaces* **2019,** *11*, 4560-4567.
(16) Bishop, L. M.; Yeager, J. C.; Chen, X.; Wheeler, J. N.; Torelli, M. D.; Benson, M. C.; Burke, S. D.; Pedersen, J. A.; Hamers, R. J. A Citric Acid-Derived Ligand for Modular Functionalization of Metal Oxide Surfaces via "Click" Chemistry. *Langmuir* **2012,** *28*, 1322-1329.
(17) Shah, S.; Benson, M. C.; Bishop, L. M.; Huhn, A. M.; Ruther, R. E.; Yeager, J. C.; Tan, Y.; Louis, K. M.; Hamers, R. J. Chemically assembled heterojunctions of SnO2 nanorods with TiO2 nanoparticles via "click" chemistry. *J. Mater. Chem.* **2012,** *22*, 11561-11567.
(18) Cao, Y.; Galoppini, E.; Reyes, P. I.; Lu, Y. Functionalization of Nanostructured ZnO Films by Copper-Free Click Reaction. *Langmuir* **2013,** *29*, 7768-7775.
(19) Palomaki, P. K. B.; Dinolfo, P. H. A Versatile Molecular Layer-by-Layer Thin Film Fabrication Technique Utilizing Copper(I)-Catalyzed Azide-Alkyne Cycloaddition. *Langmuir* **2010,** *26*, 9677-9685.
(20) Topka, M. R.; Dinolfo, P. H. Synthesis, Characterization, and Fluorescence Properties of Mixed Molecular Multilayer Films of BODIPY and Zn(II) Tetraphenylporphyrins. *ACS Appl. Mater. Interfaces* **2015,** *7*, 8053-8060.
(21) Pati, P. B.; Zhang, L.; Philippe, B.; Fernández-Terán, R.; Ahmadi, S.; Tian, L.; Rensmo, H.; Hammarström, L.; Tian, H. Insights into the Mechanism of a Covalently-Linked Organic Dye-Cobaloxime Catalyst System for Dye Sensitized Solar Fuel Devices. *ChemSusChem* **2017,** *10*, 2480–2495.
(22) Sahara, G.; Kumagai, H.; Maeda, K.; Kaeffer, N.; Artero, V.; Higashi, M.; Abe, R.; Ishitani, O. Photoelectrochemical Reduction of CO2 Coupled to Water Oxidation Using a Photocathode with a Ru(II)–Re(I) Complex Photocatalyst and a CoOx/TaON Photoanode. *J. Am. Chem. Soc.* **2016,** *138*, 14152-14158.
(23) Kaeffer, N.; Massin, J.; Lebrun, C.; Renault, O.; Chavarot-Kerlidou, M.; Artero, V. Covalent Design for Dye-Sensitized H2-Evolving Photocathodes Based on a Cobalt Diimine–Dioxime Catalyst. *J. Am. Chem. Soc.* **2016,** *138*, 12308-12311.

(24) Ashford, D. L.; Lapides, A. M.; Vannucci, A. K.; Hanson, K.; Torelli, D. A.; Harrison, D. P.; Templeton, J. L.; Meyer, T. J. Water Oxidation by an Electropolymerized Catalyst on Derivatized Mesoporous Metal Oxide Electrodes. *J. Am. Chem. Soc.* **2014,** *136*, 6578-6581.
(25) Lapides, A. M.; Ashford, D. L.; Hanson, K.; Torelli, D. A.; Templeton, J. L.; Meyer, T. J. Stabilization of a Ruthenium(II) Polypyridyl Dye on Nanocrystalline TiO2 by an Electropolymerized Overlayer. *J. Am. Chem. Soc.* **2013,** *135*, 15450-15458.
(26) Wu, L.; Brennaman, M. K.; Nayak, A.; Eberhart, M.; Miller, A. J. M.; Meyer, T. J. Stabilization of Ruthenium(II) Polypyridyl Chromophores on Mesoporous TiO2 Electrodes: Surface Reductive Electropolymerization and Silane Chemistry. *ACS Central Sci.* **2019,** *5*, 506-514.
(27) Hanson, K.; Torelli, D. A.; Vannucci, A. K.; Brennaman, M. K.; Luo, H.; Alibabaei, L.; Song, W.; Ashford, D. L.; Norris, M. R.; Glasson, C. R. K.*, et al.* Self-Assembled Bilayer Films of Ruthenium(II)/Polypyridyl Complexes through Layer-by-Layer Deposition on Nanostructured Metal Oxides. *Angew. Chem. Int. Ed.* **2012,** *51*, 12782-12785.
(28) Materna, K. L.; Lalaoui, N.; Laureanti, J. A.; Walsh, A. P.; Rimgard, B. P.; Lomoth, R.; Thapper, A.; Ott, S.; Shaw, W. J.; Tian, H.*, et al.* Using Surface Amide Couplings to Assemble Photocathodes for Solar Fuel Production Applications. *ACS Appl. Mater. Interfaces* **2020,** *12*, 4501-4509.
(29) Materna, K. L.; Beiler, A. M.; Thapper, A.; Ott, S.; Tian, H.; Hammarstroem, L. Understanding the Performance of NiO Photocathodes with Alkyl-Derivatized Cobalt Catalysts and a Push-Pull Dye. *ACS Appl. Mater. Interfaces* **2020,** *12*, 31372-31381.
(30) Bentounsi, Y.; Seintis, K.; Ameline, D.; Diring, S.; Provost, D.; Blart, E.; Pellegrin, Y.; Cossement, D.; Vauthey, E.; Odobel, F. Chemistry on the electrodes: post-functionalization and stability enhancement of anchored dyes on mesoporous metal oxide photoelectrochemical cells with copper-free Huisgen cycloaddition reaction. *J. Mater. Chem. A* **2020,** *25*, 12633-12640.
(31) Gibson, E. A.; Smeigh, A. L.; Pleux, L. L.; Fortage, J.; Boschloo, G.; Blart, E.; Pellegrin, Y.; Odobel, F.; Hagfeldt, A.; Hammarström, L. A p-Type NiO-based Dye-Sensitized Solar Cell with a Voc of 0.35 V. *Angew. Chem. Int. Ed.* **2009,** *48*, 4402-4405.
(32) Odobel, F.; Pellegrin, Y.; Gibson, E. A.; Hagfeldt, A.; Smeigh, A. L.; Hammarström, L. Recent advances and future directions to optimize the performances of p-type dye-sensitized solar cells. *Coord. Chem. Rev.* **2012,** *256*, 2414-2423.
(33) Morandeira, A.; Fortage, J.; Edvinsson, T.; Le Pleux, L.; Blart, E.; Boschloo, G.; Hagfeldt, A.; Hammarström, L.; Odobel, F. Improved Photon-to-Current Conversion Efficiency with a Nanoporous p-Type NiO Electrode by the Use of a Sensitizer-Acceptor Dyad. *J. Phys. Chem. C* **2008,** *112*, 1721-1728.
(34) Farré, Y.; Zhang, L.; Pellegrin, Y.; Planchat, A.; Blart, E.; Boujtita, M.; Hammarström, L.; Jacquemin, D.; Odobel, F. Second Generation of Diketopyrrolopyrrole Dyes for NiO-Based Dye-Sensitized Solar Cells. *J. Phys. Chem. C* **2016,** *120*, 7923-7940.
(35) Tian, D.; Zhang, H.-Z.; Zhang, D.-S.; Chang, Z.; Han, J.; Gao, X.-P.; Bu, X.-H. Li-ion storage and gas adsorption properties of porous polyimides (PIs). *RSC Advances* **2014,** *4*, 7506-7510.
(36) Wood, C. J.; Summers, G. H.; Clark, C. A.; Kaeffer, N.; Braeutigam, M.; Carbone, L. R.; D'Amario, L.; Fan, K.; Farre, Y.; Narbey, S.*, et al.* A comprehensive comparison of dye-sensitized NiO photocathodes for solar energy conversion. *Phys. Chem. Chem. Phys.* **2016,** *18*, 10727-10738.
(37) Renaud, A.; Chavillon, B.; Cario, L.; Pleux, L. L.; Szuwarski, N.; Pellegrin, Y.; Blart, E.; Gautron, E.; Odobel, F.; Jobic, S. Origin of the Black Color of NiO Used as Photocathode in p-Type Dye-Sensitized Solar Cells. *J. Phys. Chem. C* **2013,** *117*, 22478-22483.
(38) Aster, A.; Licari, G.; Zinna, F.; Brun, E.; Kumpulainen, T.; Tajkhorshid, E.; Lacour, J.; Vauthey, E. Tuning symmetry breaking charge separation in perylene bichromophores by conformational control. *Chem. Sci.* **2019,** *10*, 10629-10639.
(39) Lang, B.; Mosquera-Vazquez, S.; Lovy, D.; Sherin, P.; Markovic, V.; Vauthey, E. Broadband Ultraviolet-Visible Transient Absorption Spectroscopy in the Nanosecond to Microsecond Time Domain with Sub-Nanosecond Time Resolution. *Rev. Sci. Instrum.* **2013,** *84*, 073107-8.
(40) van Stokkum, I. H. M.; Larsen, D. S.; van Grondelle, R. Global and Target Analysis of Time-Resolved Spectra. *Biochim. Biophys. Acta, Bioenerg.* **2004,** *1657*, 82-104.

(41) Beckwith, J. S.; Rumble, C. A.; Vauthey, E. Data analysis in transient electronic spectroscopy – an experimentalist's view. *Int. Rev. Phys. Chem.* **2020,** *39*, 135-216.
(42) Kim, T.; Kim, W.; Vakuliuk, O.; Gryko, D. T.; Kim, D. Two-Step Charge Separation Passing Through the Partial Charge-Transfer State in a Molecular Dyad. *J. Am. Chem. Soc.* **2020,** *142*, 1564-1573.
(43) Gosztola, D.; Niemczik, M. P.; Svec, W.; Lukas, A. S.; Wasielewski, M. R. Excited Doublet States of Electrochemically Generated Aromatic Imide and Diimide Radical Anions. *J. Phys. Chem. A* **2000,** *104*, 6545-6551.
(44) Gibson, E. A.; Smeigh, A. L.; Le Pleux, L.; Hammarström, L.; Odobel, F.; Boschloo, G.; Hagfeldt, A. Cobalt Polypyridyl-Based Electrolytes for p-Type Dye-Sensitized Solar Cells. *J. Phys. Chem. C* **2011,** *115*, 9772-9779.
(45) Odobel, F.; Pellegrin, Y.; Warnan, J. Bio-inspired artificial light-harvesting antennas to enhance solar energy capture in dye-sensitized solar cells. *Energy Environ. Sci.* **2013,** *6*, 2041-2052.

Click chemistry on NiO photocathode to post-functionalize a diketopyrrolopyrrole sensitizer by naphthalene diimide electron acceptor

Yousra Bentounsi,[a] Konstantinos Seintis,[b] Stéphane Diring,[a] Eric Vauthey[b] Fabrice Odobel*[a]*

[a]Université de Nantes, CNRS, CEISAM UMR 6230, F-44000 Nantes, France. E-mail: Fabrice.Odobel@univ-nantes.fr

Department of Physical Chemistry, University of Geneva, 30 Quai Ernest-Ansermet, CH-1211 Geneva, Switzerland. E-mail: Eric.Vauthey@unige.ch